SCIENCE CHINA
Earth Sciences

•RESEARCH PAPER•

June 2019 Vol.62 No.6: 953–963
https://doi.org/10.1007/s11430-018-9327-1

A 1556 year-long early summer moisture reconstruction for the Hexi Corridor, Northwestern China

Bao YANG*, Jianglin WANG & Jingjing LIU

Key Laboratory of Desert and Desertification, Northwest Institute of Eco-Environment and Resources, Chinese Academy of Sciences, Lanzhou 730000, China

Received September 30, 2018; revised December 10, 2018; accepted January 4, 2019; published online March 14, 2019

Abstract We report a 1556 year-long tree-ring width chronology for the Hexi Corridor, in the arid Northwestern China, established by applying the signal-free regional curve standardization method to 416 juniper ring-width series. We found that drought in early summer (May–June) is the primary controlling factor for tree growth in this area. We then developed an early summer moisture (i.e., scPDSI) reconstruction from 455 CE to present. Our reconstruction captures multi-centennial scale moisture variations, showing two long-term dry periods during 800–950 CE and 1000–1200 CE, and two long-term wet periods during 1200–1450 CE and 1510–1620 CE. We found strong similarities between hydroclimatic changes in the Hexi Corridor and Qaidam Basin from interannual to centennial timescales; however, at multi-centennial (>300 years) timescales, hydroclimatic variations in the two regions showed significant regional differences. The Hexi Corridor witnessed a generally dry Medieval Climate Anomaly (MCA, here 800–1200 CE) and the drying 20th century, whereas the Qaidam Basin experienced high-precipitation periods during the MCA and 20th century. The different correlation pattern with Northern Hemisphere temperature suggest that the Qaidam Basin will receive more precipitation under global warming, whereas the Hexi Corridor will become dryer in the future.

Keywords Hexi Corridor, Tree-ring index, Early-summer, Hydroclimate reconstruction

Citation: Yang B, Wang J, Liu J. 2019. A 1556 year-long early summer moisture reconstruction for the Hexi Corridor, Northwestern China. Science China Earth Sciences, 62: 953–963, https://doi.org/10.1007/s11430-018-9327-1

1. Introduction

Evidence from observations suggests that global warming is accompanied by an increasing frequency and severity of droughts, as well as accelerated dry-land expansion, which threaten both the environment and society (Dai, 2013; Huang et al., 2015, 2017). Furthermore, it is suggested that more frequent and widespread droughts will occur in the next decades as a result of global warming increased evaporation (Cook et al., 2015; Dai, 2013). Droughts have repeatedly affected large populations, with the most negative consequences occurring in arid and semi-arid areas during the past millennia. Northwestern China is a typical arid region of central Asia, accounting for about 30 percent of China's total territory. Drought is one of the most devastating natural disasters affecting the people living in these ecologically vulnerable regions. For example, the severe drought in northern China in the 1920s and related famines and diseases led to the death of about four million residents (Xu et al., 1997). In contrast, with droughts lasting several years, a mega-drought that lasts decades to centuries might constitute one of the most serious threats to human welfare. Such mega-droughts have been temporally associated with major cultural imprints in China (Zhang et al., 2008), Mongolia (Pederson et al., 2014), Cambodia (Buckley et al., 2010) and Europe (Büntgen et al., 2011).

* Corresponding author (email: yangbao@lzb.ac.cn)

© Science China Press and Springer-Verlag GmbH Germany, part of Springer Nature 2019

Our knowledge of the characteristics of historical droughts has been largely dependent on paleoclimate proxy records. As a widely used paleoclimate proxy, tree rings from drought sensitive sites provide annually resolved climate records covering centuries or even millennia (Fritts, 1976). The Hexi Corridor, located in a typically arid and semi-arid region of northwestern China, is an ideal sampling site to research dendroclimatology, yet very few dendrochronological studies have focused on this region (Chen et al., 2013; Liang et al., 2009; Liu et al., 2016; Tian et al., 2007); the tree-ring records in these studies only span time scales shorter than 250 years that are insufficient to reveal climate variability on centennial timescales. In a previous study, we reported a 620 year-long precipitation reconstruction derived from 56 tree-ring samples in the Hexi Corridor in the arid northwest China (Yang et al., 2011). Thereafter, Gou et al. (2015b) extended the chronology to 850 years before present. Nevertheless, it may be possible to extend it further, potentially even over the past millennium.

Many studies have focused on the medieval hydroclimate anomalies and suggested a global mega-drought during the medieval period (Diaz et al., 2011; Graham et al., 2010). However, we still know little about hydroclimatic conditions in the arid northwest China during the medieval period, due to lack of accurately dated proxy records, and ambiguous hydroclimate signals. During the past few years, we have collected a large number of tree-ring samples in this region, which increases our confidence in constructing a long-term ring-width chronology covering the entire Medieval Climate Anomaly (MCA, here 800–1200 CE) and the Little Ice Age (LIA, here 1400–1900 CE) (Yang et al., 2002). In this study, we report a 1556 year-long ring-width chronology for the Hexi Corridor, using the Signal-Free Regional Curve Standardization (SF-RCS) methodology to calculate a chronology based on 416 Qilian juniper ring-width samples. We use this ring-width chronology to reconstruct the May–June mean scPDSI (self-calibrating Palmer Drought Severity Index) over the past 1556 years. This is the first millennium-long, annually-resolved hydroclimate reconstruction for the Hexi Corridor.

2. Materials and methods

2.1 Tree-ring data

Increment cores of Qilian juniper (*Sabina przewalskii* Kom.) were systematically collected during the 2007–2012 summers from trees growing in juniper forests in Qifeng town, Jiuquan city, Gansu Province, China (Figure 1). The forests selected for sampling comprise open stands at elevations between 3000 and 3520 m a.s.l (meter above sea level). In total, 435 cores from 243 trees were sampled, including the 56 cores from 31 trees which were used to develop the ring-width chronology in our previous study (Yang et al., 2011). The ring widths of each tree core were measured to 0.01 mm accuracy using the LINTAB measuring system. The tree-ring sequences were cross-dated using visual growth pattern matching and statistical tests in the software package TSAP-Win. The cross-dated tree-ring series were quality checked with COFECHA software (Holmes, 1983). Ring-width series with poor correlation with the master series, due to either age-related trends or different local habitats, were removed. Ultimately, 416 increment cores from 233 trees were included for analysis. The previous study suggested that tree growth at different elevation bands in this site is mainly controlled by moisture, despite the large altitudinal gradient (520 m) from the lower to upper treelines (Yang et al., 2013). Consequently, ring-width samples from all elevation bands were used to produce chronologies.

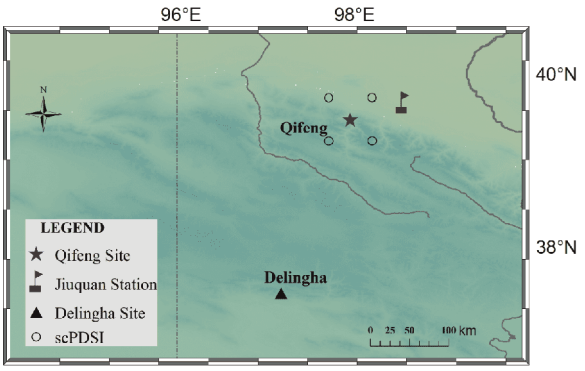

Figure 1 Locations of the sampling sites (stars), the meteorological station (flag), the scPDSI grid points (circles), and the tree-ring sampling site in the Qaidam Basin (triangle; Yang et al, 2014).

2.2 Chronology development

The traditional standard chronology (STD) was calculated using the ARSTAN program (Cook, 1985). The variance of each series was stabilized using a data-adaptive power transformation based on the local mean and standard deviation before calculating the final chronology (Cook and Peters, 1997). A modified negative exponential curve (any k) was used to fit to the raw ring-width series to remove age-related biological trends. The tree-ring sequences were then detrended with a cubic smoothing spline function with a 50% frequency-response cutoff equal to 67% of the series length. The tree-ring chronology was calculated using the residuals between the raw measurements and the fitted values. The Expressed Population Signal (EPS) was calculated to determine the most reliable period by using a 30-year moving window with 15-year overlaps (Wigley et al., 1984). The reliable chronology period extended back to 455 CE, with at least 5 trees and an EPS >0.85.

It should be noted that the STD method may remove low-frequency climate signals on timescales equal to two thirds

of the mean length of tree-ring series (Cook et al., 1995). The Regional Curve Standardization (RCS) detrending technique is an effective method of retaining low-frequency variations (Briffa and Melvin, 2011; Esper et al., 2003; Melvin and Briffa, 2008); however, RCS is sensitive to the influence of non-climate-related factors that may bias the tree-ring chronologies. The "trend-in-signal" bias resulting from the removal of non-climate-related variance is most prevalent at the ends of the RCS chronologies (Briffa and Melvin, 2011; Melvin and Briffa, 2008). The term ''trend distortion'' was used by Melvin and Briffa (2008) to describe this effect, and they reported the "signal-free" standardization approach to mitigate the trend distortion problem. In this paper, the signal-free (SF-) RCS method was adopted by applying the software tool CRUST (Melvin and Briffa, 2014), as we have in previous works (Wang et al., 2014).

2.3 Climate data

Monthly temperature and precipitation data since 1951 CE from the nearest meteorological station Jiuquan (39°46′N, 98°29′E, 1477 m) were used to investigate the relationship between tree-growth and climate. The mean annual temperature during 1951–2011 CE was 7.48°C. January and July are the coldest and warmest months, with mean temperatures of –9.43°C and 21.98°C, respectively. Mean annual precipitation is 87 mm for the period 1951–2011, about eighty percent of which falls during the summer months from May to September.

The scPDSI was used as a drought indicator (van der Schrier et al., 2013). The PDSI is a metric of meteorological drought, and has been proven suitable for describing moisture conditions across western China (Fang et al., 2009; Kang et al., 2012; Li et al., 2008, 2017). The scPDSI is a modified metric of the PDSI and is especially suitable for regions with diverse climatology (van der Schrier et al., 2013). We used an average series of four half-degree scPDSI grid points close to our sampling site to represent regional moisture conditions over the period 1951–2011.

3. Results and discussion

3.1 Chronology characteristics

Figure 2a presents the mean ring-width and the age-aligned regional growth curve for the SF-RCS standardization based on 416 ring-width samples. The regional growth curve showed a regular distribution around the mean ring width. Unusually, a decrease in mean ring-width was seen over the first ten years, but the width then increases over the next decades. This may be a result of not considering pith offset information in the ring-width samples (Esper et al., 2003). It has been suggested that missing pith offset information can affect the alignment of ring-width data by affecting biological (cambial) age and the position of the regional curve used for the detrending of all ring-width series (Esper et al., 2003).

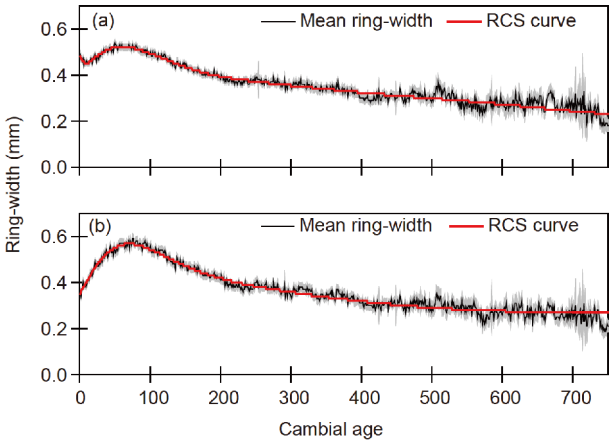

Figure 2 Two age-aligned, Signal-Free RCS curves for all 416 ring-width series (a) and for 269 series with pith offset (b).

To assess the effect of with or without considering pith offset information, we produced a SF-RCS chronology only using the 269 increment cores with accurate information on pith offset. The mean ring-width and regional growth curve for ring-width series with pith offset increased more stably over the first 70 years, and then showed a tiny downward trend at multi-century time scales after the earliest 200 years (Figure 2b). Comparing chronologies with and without consideration of pith offset information yields high coherence in both high- and low-frequency variations in the two SF-RCS chronologies (r=0.99, p<<0.01). This suggests that the SF-RCS chronologies produced in this study are poorly sensitive to changes in either number of series used or mean cambial age (Figure 3c and 3d; also see Wang et al. (2014) for a detailed discussion). Furthermore, the high coherence between the two SF-RCS chronologies also implies that the omission of pith offset information has no significant influence on RCS chronologies, consistent with findings in other studies (Esper et al., 2003, 2009).

The comparison between the SF-RCS and STD chronologies (Figure 3a) reveals general similarities in both trend and amplitude of variations, with a correlation coefficient of 0.92 for the reliable period 455–2011 (EPS>0.85). The major differences between the two chronologies occurred in 700–1050 and 1300–1450. It is obvious that more low-frequency variability is preserved in the RCS chronology (Figure 3a), even though the long mean segment length (~470 years) of 416 ring-width series suggests some potential preservation of multi-centennial signals in the STD chronology.

3.2 Tree growth-climate relationship

The relationship between tree growth and climate variables

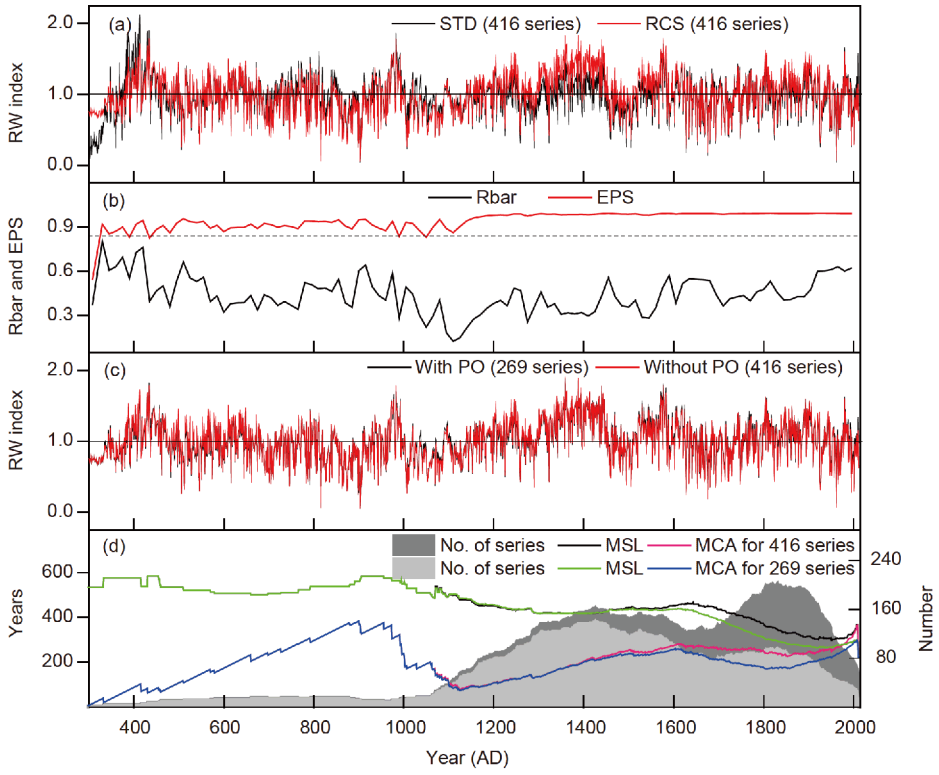

Figure 3 (a) Comparison between the signal-free regional curve standardization (SF-RCS) and traditional standard (STD) chronologies calculated from all samples (416 series). (b) 31-year running mean inter-series correlation (Rbar) and expressed population signal (EPS) statistics with critical 0.85 EPS (dotted line). (c) Comparison between two RCS chronologies calculated from all samples (416 series) and the subset of samples (269 series) with pith offset (PO). (d) Temporal variation in sample depth, mean segment length (MSL) and mean cambial age (MCA) for all samples (416 series) and the subset of samples (269 series).

was investigated in the period 1951–2011. Because of the very strong correlation (r=0.97, p<0.01) between the STD and RCS chronologies in the calibration period 1951–2011, we herein only show the analyses using the SF-RCS chronology calculated from the 416 ring-width series. Correlation coefficients between tree-growth and monthly temperature, precipitation and scPDSI were calculated from July of the previous year to September of the current year.

As shown in Figure 4, the SF-RCS chronology significantly positively correlates with the 11-month precipitation data (p<0.05) in the previous July and August and the current May and June. The highest correlation (r=0.60, p<0.01) between tree-ring chronology and precipitation is found for the annual mean from July of the previous year to June of the current year. For temperature, the SF-RCS chronology negatively correlates with eight-month temperature data, although the correlation is significant only in July of the previous year. Negative effects of high temperatures on Qilian juniper growth in the early growing season were also reported in other studies (Shao et al., 2005; Sheppard et al., 2004; Zhang et al., 2003, 2015). The positive (negative) correlations with precipitation (temperature) indicate the typical moisture stress on tree growth (Fang et al., 2015; Gou et al., 2015a; Li et al., 2017; Zhang et al., 2015).

Based on the above analysis, we examined the correlations between SF-RCS tree-ring chronology and the scPDSI during the period 1951–2011. As shown in Figure 4, significant positive correlations with the scPDSI are found in most months (14/15 months) investigated, with the highest values in early summer (May–June). This suggests that the early growing season moisture is the most critical factor limiting tree growth in the Hexi Corridor. In addition, a high correlation (r=0.48, p<0.01) is also seen for the annual mean scPDSI from July of the previous year to June of the current year. These climate-tree growth relationships indicate that our chronology is most suitable for the reconstruction of May–June scPDSI changes (r=0.63, p<0.01) in the study area.

3.3 Early summer scPDSI reconstruction

A linear regression model with a sliding window approach for calibration (2/3 length) and verification (1/3 length) (Wang et al., 2017) was used to develop the reconstruction. The initial calibration interval extended from 1951 to 1991 and was incremented by one year until reaching the final period 1971–2011, deriving an ensemble of 21 plausible reconstruction members. The scPDSI reconstruction, reduction of error (RE), coefficient of efficiency (CE) and R^2 statistics were then characterized as the median value of the

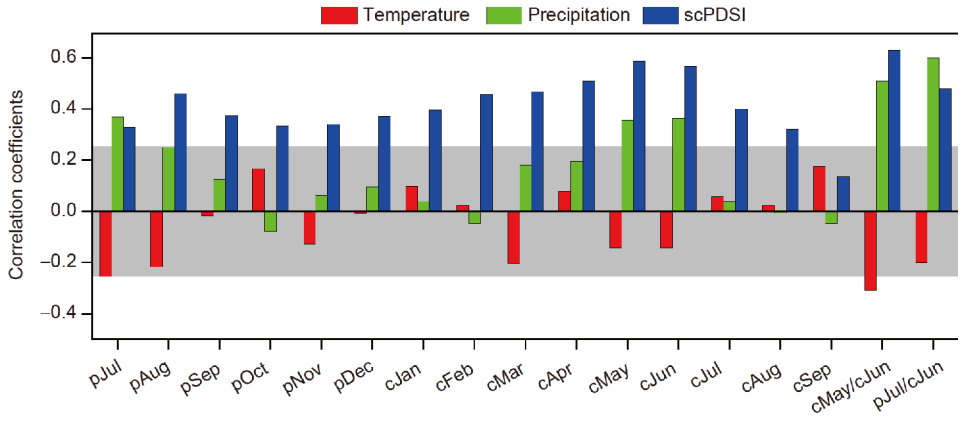

Figure 4 Correlation of the signal-free regional curve standardization (SF-RCS) chronology index with monthly precipitation (green), mean temperature (red) and scPDSI (blue) from July of the previous year to September of the current year. The 0.05 significance levels are shown by the grey shading.

21 ensemble members.

The RE, CE and R^2 in the verification period show positive values in all cases (Figure 5), indicating the reliability of the derived reconstruction (Cook et al., 1994). The reconstruction model explains 40% of the instrumental scPDSI variance during the period 1952–2011. Even though the reconstruction cannot explain the very high variance, both high- and low-frequency moisture variations are reconstructed reasonably well (Figure 6a). This is confirmed by the very strong correlation between the first order differences of actual and reconstructed values (r=0.74, p<0.01) (Figure 6b). In addition, the reconstructed values match better with real values in drought years than in pluvial years (Figure 6a), which has also been reported in other Qilian juniper sites (Sheppard et al., 2004; Zhang et al., 2011). This can be partly explained by Qilian juniper growth in pluvial years being more limited by climatic factors other than drought stress. Another reason might be that a pluvial event leads to surface runoff on the strongly inclined slopes, such that the moisture cannot be fully used by the trees for biomass production. However, such underestimation in pluvial years will not affect our interpretation of long-term trends.

Our 1556-year May–June scPDSI reconstruction shows two long-term dry periods in 800–950 CE and 1000–1200 CE and two pluvial periods in 1200–1450 CE and 1510–1620 CE (Figure 6c). Using a 30-year running mean, we detected the five driest and five wettest multidecadal periods over the entire reconstructed series. The two centennial-scale dry periods of 800–950 CE and 1000–1200 CE contained four of the five driest multidecadal droughts: 856–885 CE, 1051–1080 CE, 1004–1033 CE and 892–921 CE (in order of increasing mean values). The two centennial-scale wet periods of 1200–1450 CE and 1510–1620 CE contained four of the five wettest multidecadal pluvial periods: 1381–1410 CE, 1345–1374 CE, 1417–1446 CE and 1554–1583 CE (in order of decreasing mean values).

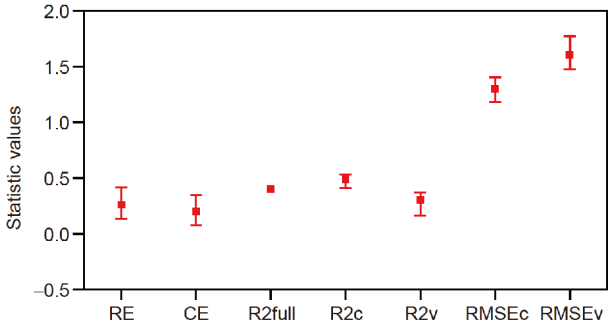

Figure 5 Statistics (10% range, median, 90% range) for the sliding calibration and verification. Reduction of error (RE), coefficient of efficiency (CE), root mean square error (RMSEv), R^2 (R2v) are for verification intervals; root mean square error (RMSEc), R^2 (R2c) are for calibration intervals; R^2 (R2full) is for the full interval 1951–2011 CE.

3.4 Comparisons with regional hydroclimate reconstructions

To investigate the regional representativeness of our reconstruction, we calculated spatial correlations between our reconstruction and the Monsoon Asia Drought Atlas (MADA) (Cook et al., 2010). As shown in Figure 7, our scPDSI reconstruction correlates significantly with the MADA PDSI reconstructions over the northeastern TP. The correlation coefficients range from 0.2 to 0.4 (p<0.01), and increase to 0.5–0.6 (p<0.01) after 11-year running averaging during the period 1300–2005 CE. Although the seasonal responses between our reconstruction and the MADA dataset are slightly different (i.e., May–June *vs.* June–August), their high correlation suggests our scPDSI reconstruction captures signals of regional inter-annual to decadal hydroclimatic variability over the northeastern TP.

We compared our reconstruction with a tree-ring based annual (July–June) precipitation reconstruction for the Qaidam Basin (Yang et al., 2014, 2017b) (Figure 8). The Qaidam

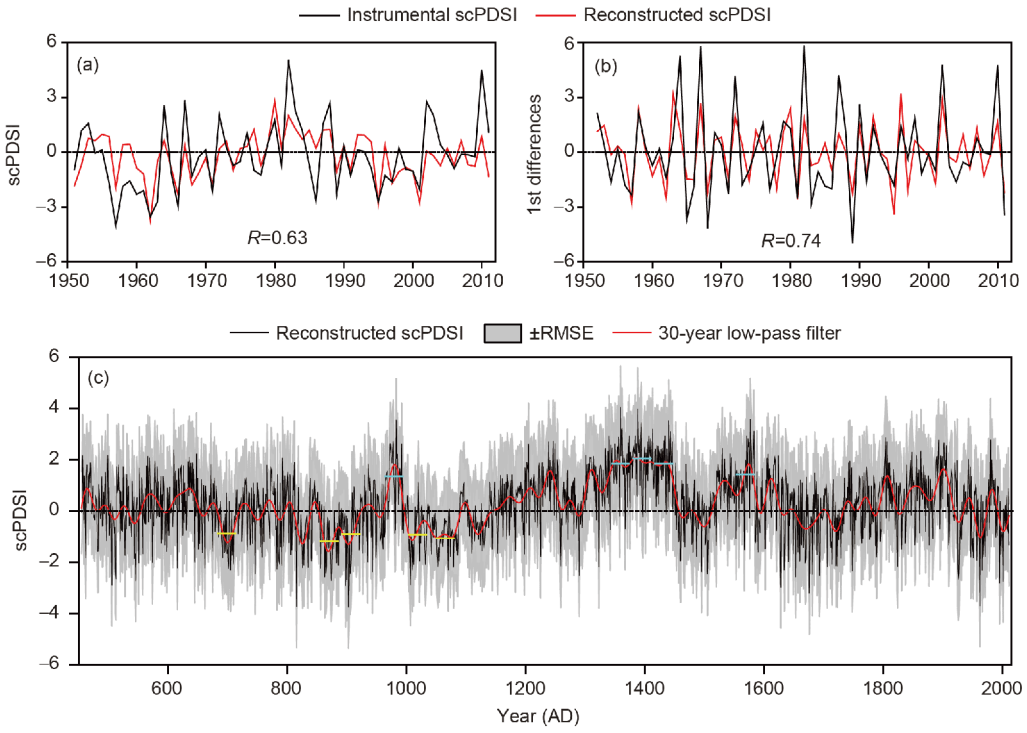

Figure 6 (a) Comparison between the reconstructed and instrumental (May–June) scPDSI. (b) Same as (a) but for their 1st differences. (c) Annually resolved scPDSI reconstruction (black), its 30-year low pass filter (red), as well as the ±1 root mean square error (RMSE) uncertainties for verification (gray shades).

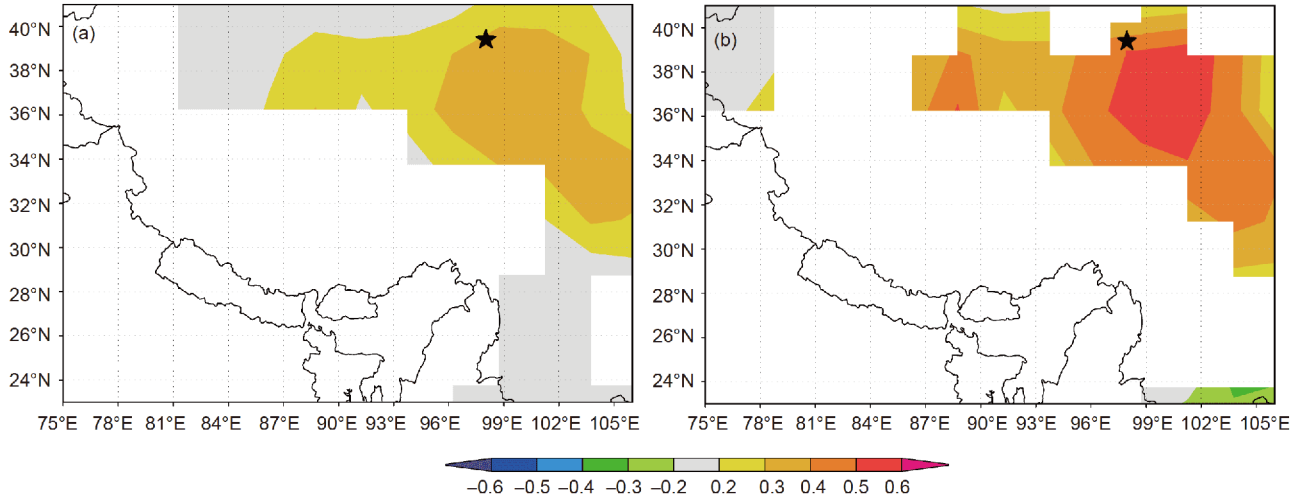

Figure 7 (a) Spatial correlation patterns between the reconstructed May–June scPDSI and June-August monsoon Asia drought atlas (MADA) PDSI dataset (Cook et al., 2010) over the period 1300–2005 CE. (b) Same as (a) but for the 11-year running mean data. Only correlation coefficients that are significant at the 0.05 level are shown here. The sample site for this study is marked by the star.

hydroclimate reconstruction has strong regional representativeness, as it shows similar variation patterns to those of other hydroclimate reconstructions in this region (see discussion in Yang et al. (2014) and Yin et al. (2016)). The two hydroclimate reconstructions show generally coherence over the common period 455–2011 with a correlation coefficient of r=0.30 (p<0.01). The two reconstructions reveal common multi-decadal wet conditions during the periods 1210–1250 CE, 1310–1420 CE and 1530–1620 CE, and dry conditions during the periods 1100–1160 CE, 1430–1520 CE and 1660–1730 CE. These wet/dry events revealed by the two tree-ring records are generally consistent with the low/high dust concentration periods recorded in the Dunde ice core (Mosley-Thompson et al., 1993). In addition, the generally wet conditions in the Hexi Corridor during the LIA are consistent with previous interpretations of climate in arid

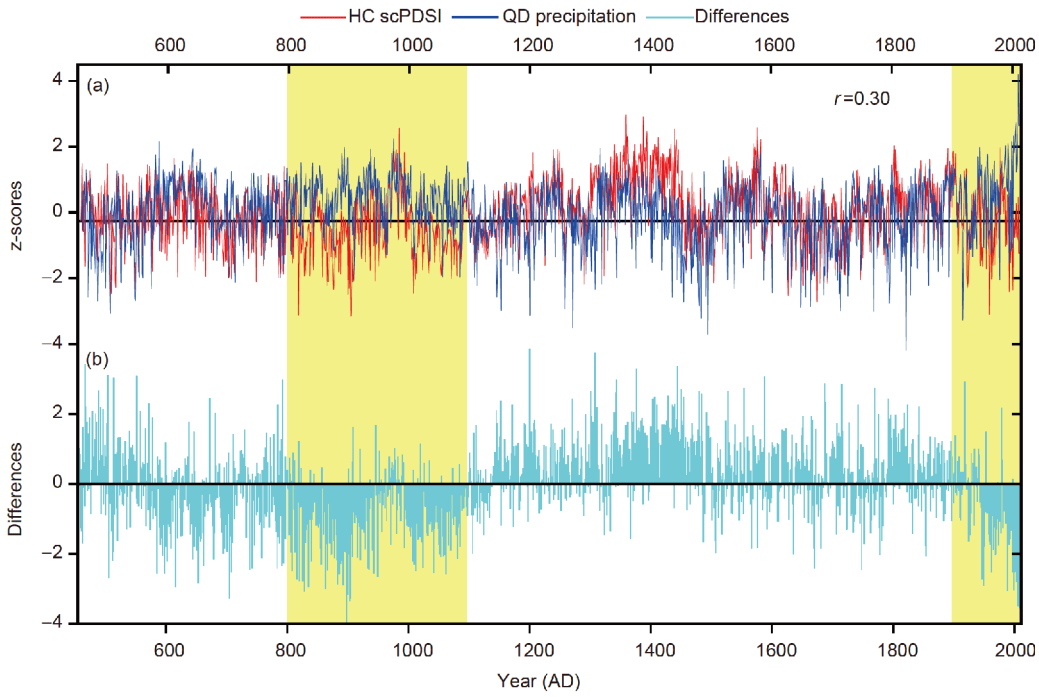

Figure 8 (a) Comparison between the May–June scPDSI reconstruction for the Hexi Corridor (HC, red) and the July–June precipitation reconstruction for the Qaidam Basin (QB, blue; Yang et al. (2014)). (b) The differences between the two normalized hydroclimatic reconstructions.

central Asia (Chen et al., 2015).

The major discrepancies are also obvious in the long-term behaviors of the two hydroclimatic reconstructions: these are during medieval times and the 20th century. During the 20th century, the eastern Qaidam Basin experienced increasing tree growth and pluvial conditions, whereas the Hexi Corridor witnessed decreasing tree growth and drying conditions. The increasing tree growth during the 20th century across the Qaidam Basin was also observed in other studies (Liu et al., 2006; Shao et al., 2010; Sheppard et al., 2004; Zhang et al., 2015), and the decreasing tree growth in the Hexi Corridor was also reported in other studies (Deng et al., 2012; Liang et al., 2016a). During the 9th–11th centuries, our reconstruction reveals prolonged dry conditions, whereas the Qaidam Basin reconstruction shows long-term wet (high-precipitation) conditions (Figure 8). Note that a prolonged drought is still evident in the Hexi Corridor reconstruction if we use a traditional method to calculate tree-ring chronology. It is worth noting that the two major differences were coincident with the Northern Hemisphere warm periods during the MCA (800–1200 CE) and the 20th century (Anchukaitis et al., 2017; Ljungqvist et al., 2012, 2016; Wilson et al., 2016; Yang et al., 2002), suggesting a possible role of temperature in causing the differences between the two hydroclimate reconstructions.

3.5 Comparisons with NH temperature reconstruction

The Ensemble Empirical Mode Decomposition (EEMD; Huang et al. (1998); Wu and Huang (2009)) was used to decompose the reconstructions of scPDSI for the Hexi corridor, of precipitation for the Qaidam Basin, and of temperature for the Northern Hemisphere, to several intrinsic mode functions from interannual to multi-centennial timescales over the common period 755–2011 CE (Figure 9). Significantly positive correlations could be seen between the two hydroclimate reconstructions for the Hexi Corridor and for the Qaidam Basin from interannual to centennial timescales (Figure 10); however, at multi-centennial (>300 years) timescales, the two hydroclimate records are negatively correlated, although not significantly at the 0.05 significance level. In addition, the correlation between the Qaidam Basin precipitation and the NH temperature is positive at all timescales, with the strongest correlation at multi-centennial timescales (r=0.76, p<0.05), consistent with our previous finding (Yang et al., 2014), and also points to a co-variability of temperature and precipitation in the Qaidam Basin during the past two millennia.

Compared to the Qaidam Basin hydroclimate, we find the correlations between the the Hexi Corridor scPDSI and the NH temperature are generally weak through most timescales (Figure 10). In particular, we find that the relationships between the Hexi Corridor scPDSI and NH temperature are weaker and even negative for the longer (e.g., centennial and multi-centennial) timescales over the period 755–2011 CE. The weak negative correlation (r=−0.22, p<0.1) is also seen between early summer (May–June) temperature and precipitation at Jiuquan station during the period 1951–2011

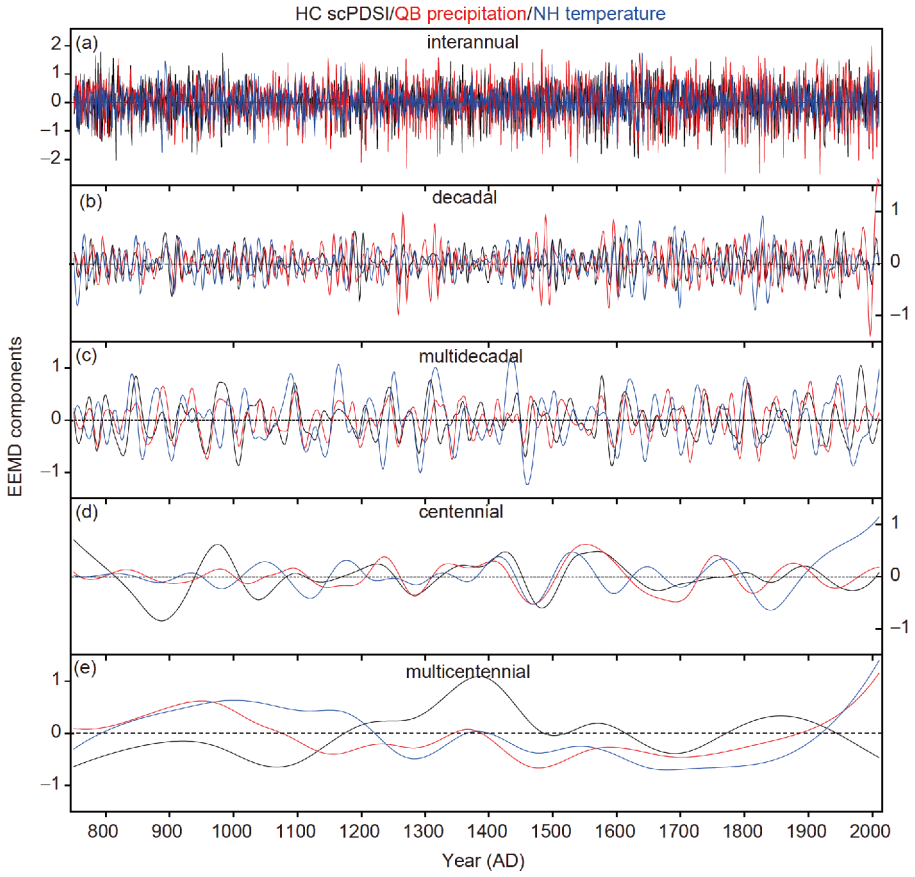

Figure 9 The intrinsic mode functions of the May–June scPDSI reconstruction for the Hexi Corridor (HC, black; this study), the July–June precipitation reconstruction for the Qaidam Basin (QB, red; Yang et al. (2014)), and the May–September temperature reconstruction for the Northern Hemisphere (NH, blue; Wilson et al. (2016)).

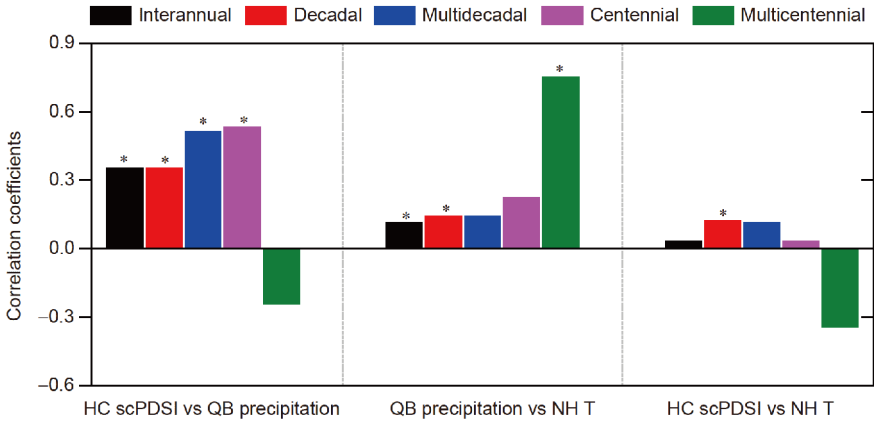

Figure 10 Correlation coefficients between the Hexi Corridor (HC) scPDSI, the Qaidam Basin (QB) precipitation and the Northern Hemisphere (NH) temperature for their intrinsic mode functions at different timescales as in Figure 9. In each case, the degrees of freedom were adjusted following Wang et al. (2017), and significant correlations at 0.05 are marked with an asterisk.

CE. The negative relationships between the scPDSI reconstruction and NH temperature are especially strong during the MCA and 20th century at multi-centennial timescales (Figure 9d); however, the positive relationships between Qaidam Basin hydroclimate and NH temperature are stable and strong during the two warm periods.

The larger differences between the two tree-ring records during the MCA and the 20th century are related to differential responses of tree growth to temperature change. Both periods are typically characterized by higher temperatures (Yang et al., 2002). In the Qaidam Basin, the reconstructed annual precipitation (prior July to current June) accounts for 70.56% of instrumental precipitation variance over the calibration period 1956–2011 (Yang et al., 2014), whereas the

tree-ring chronology for the Hexi Corridor explains only 36% of the same annual water year precipitation variance during the instrumental period. This implies that tree growth in the Qaidam Basin is much more sensitive to precipitation than that in the Hexi Corridor. Indeed, previous analysis showed that the ring-width chronology for the Hexi Corridor has the highest correlation with early summer (May–June) scPDSI. In other words, tree growth in the Hexi Corridor is mainly controlled by a combination of temperature and precipitation, whereas temperature plays a much more important role in tree growth in this region than in the Qaidam Basin. This argument is supported by the stable oxygen isotope evidence. Tree-ring δ^{18}O data are significantly negatively correlated with relative humidity in both the Qaidam Basin (Wang et al., 2013) and Hexi Corridor (Li et al., 2018). Similar to the scPDSI, relative humidity is a result of interaction between temperature and precipitation. Both tree-ring δ^{18}O chronologies show obvious increasing trends during the 20th century, indicating that both regions witnessed the drying trends in the latest 100 years. The centennial drought trend corresponds to reduced tree growth in the Hexi Corridor but is contrary to the increased tree growth in the Qaidam Basin. This provides robust evidence that temperature predominantly responsible for the large difference in tree growth (moisture variations) during the 20th century. Since the MCA represents warm conditions, it is expected that the response of tree growth to climatic change is much the same as that in the 20th century. The negative effect of temperature will be especially strong during much warmer climate regimes because of an increased risk and severity of droughts, as well as accelerated dry land expansion accompanying high temperatures (Dai, 2013; Huang et al., 2017). This inference is consistent with our dendrometer monitoring studies in the middle of the Hexi Corridor (Wang et al., 2012). In this region, we found that intra-annual variability in radial growth of Qilian juniper is mainly controlled by moisture conditions, and the growing season temperature has a negative influence on Qilian juniper growth in the middle of the Hexi Corridor (Wang et al., 2012, 2015). Meanwhile, in the Qaidam Basin, tree growth is suggested to be controlled by precipitation, and the temperature during the pre-growing season (prior September to current April) can even have a positive effect on tree-growth (Qin et al., 2013; Yang et al., 2014).

The differences in correlation pattern between the two tree-ring records are noted at various timescales (Figure 10). As we stated above, tree growth in the Qaidam Basin is predominantly controlled by precipitation whereas tree growth in the Hexi Corridor is limited by a combination of temperature and precipitation, although drought stress is a common limiting factor for tree growth in both regions. As a result, significant positive correlation (p<0.05) is found between the two tree-ring records on shorter timescales from interannual to centennial, but a weak negative correlation is seen at the multi-centennial timescale which is related to the prolonged warmer climate regimes such as the MCA and the 20th century: this is due to increased evapotranspiration and resultant drought stress in these arid regions. A multi-century (>300 years) running mean or low-pass filter effectively smooths out the short-term (<100 years) and high-frequency fluctuations of the original data and yields a negative correlation, compared to the positive correlations between the two tree-ring chronologies on shorter timescales. Similarly, it should be noted that the correlation at multi-centennial timescales is weak and not statistically significant at the 0.05 level.

The differential responses of tree growth to climatic change in the Hexi Corridor and Qaidam Basin found here may draw important implications for future alpine forest dynamics across western China. For example, the negative response of tree growth to temperature in the Hexi Corridor suggests that forest productivity may continue to reduce as a consequence of global warming. The alpine forest health in the Hexi Corridor may face greater challenges, as it will be increasingly at risk of greater tree mortality caused by temperature increases of 2 or 3°C by the end of the 21st century (Liang et al., 2016a, 2016b). Tree mortality was suggested to have a lag of several years in its response to warming-related drought in the Hexi Corridor (Liang et al., 2016a), suggesting more serious challenges in tree health in the next decades or centuries. In contrast, the positive correlation of tree growth and temperature in the Qaidam Basin suggests that alpine forest productivity may continue to increase as a consequence of global warming. This inference is consistent with our recent findings in this region, where higher temperature is always associated with increased precipitation (Yang et al., 2014) and may extend the length of the growing season (Yang et al., 2017a).

4. Conclusion

We calculated a 1556 year-long ring-width chronology by applying the SF-RCS detrending method to 416 Qilian juniper ring-width series in the Hexi Corridor, northwestern China. We found the early-summer scPDSI is the most important factor controlling tree growth in this area. We developed a May–June scPDSI reconstruction covering the period 455–2011 CE. Our reconstruction explains more than 40% of the observed moisture variance over the period 1951–2011 CE, and shows two multi-centennial droughts during 800–950 CE and 1000–1200 CE, and two multi-centennial pluvial periods during 1200–1450 CE and 1510–1620 CE. The regional comparison indicates generally coherent changes of moisture over the northeastern TP at interannual to centennial timescales. The Hexi Corridor and

Qaidam Basin experienced common multi-decadal wet conditions in 1210–1250 CE, 1310–1420 CE and 1530–1620 CE, and common dry conditions in 1100–1160 CE, 1430–1520 CE and 1660–1730 CE. Moreover, the comparison also reveals regional differences in tree growth at multi-centennial timescales between the two regions: specifically, the Hexi Corridor witnessed the reduced tree growth during the MCA and 20th century, whereas the Qaidam Basin experienced the increased tree growth during the same periods.

Acknowledgements *We thank the two anonymous reviewers who helped to improve the manuscript with insightful comments. This study was supported by the National Key R & D Program of China (Grant No. 2017YFA0603302), the National Natural Science Foundation of China (Grant Nos. 41520104005, 41602192, 41325008 & 41402157), and the Belmont Forum and JPI-Climate Collaborative Research Action 'INTEGRATE' (Grant No. 41661144008). Jianglin Wang also acknowledges the support of the Innovation Promotion Association Foundation of CAS, and the CAS "West Light" Program.*

References

Anchukaitis K J, Wilson R, Briffa K R, Büntgen U, Cook E R, D'Arrigo R, Davi N, Esper J, Frank D, Gunnarson B E, Hegerl G, Helama S, Klesse S, Krusic P J, Linderholm H W, Myglan V, Osborn T J, Zhang P, Rydval M, Schneider L, Schurer A, Wiles G, Zorita E. 2017. Last millennium Northern Hemisphere summer temperatures from tree rings: Part II, spatially resolved reconstructions. Quat Sci Rev, 163: 1–22

Büntgen U, Tegel W, Nicolussi K, McCormick M, Frank D, Trouet V, Kaplan J O, Herzig F, Heussner K U, Wanner H, Luterbacher J, Esper J. 2011. 2500 years of European climate variability and human susceptibility. Science, 331: 578–582

Briffa K R, Melvin T M. 2011. A closer look at regional curve standardization of tree-ring records: Justification of the need, a warning of some pitfalls, and suggested improvements in its application. In: Hughes M K, Diaz H F, Swetnam T W, eds. Dendroclimatology: Progress and Prospects. New York: Springer

Buckley B M, Anchukaitis K J, Penny D, Fletcher R, Cook E R, Sano M, Canh Nam L, Wichienkeeo A, That Minh T, Hong T M. 2010. Climate as a contributing factor in the demise of Angkor, Cambodia. Proc Natl Acad Sci USA, 107: 6748–6752

Chen F, Yuan Y, Wei W, Zhang R, Yu S, Shang H, Zhang T, Qin L, Wang H, Chen F. 2013. Tree-ring-based annual precipitation reconstruction for the Hexi Corridor, NW China: Consequences for climate history on and beyond the mid-latitude Asian continent. Boreas, 42: 1008–1021

Chen J, Chen F, Feng S, Huang W, Liu J, Zhou A. 2015. Hydroclimatic changes in China and surroundings during the medieval climate anomaly and Little Ice Age: Spatial patterns and possible mechanisms. Quat Sci Rev, 107: 98–111

Cook B I, Ault T R, Smerdon J E. 2015. Unprecedented 21st century drought risk in the American Southwest and central plains. Sci Adv, 1: e1400082

Cook E. 1985. A time-series analysis approach to tree-ring standardization. Doctoral Dissertation. Tucson: The University of Arizona

Cook E R, Anchukaitis K J, Buckley B M, D'Arrigo R D, Jacoby G C, Wright W E. 2010. Asian monsoon failure and megadrought during the last millennium. Science, 328: 486–489

Cook E R, Briffa K R, Jones P D. 1994. Spatial regression methods in dendroclimatology: A review and comparison of two techniques. Int J Climatol, 14: 379–402

Cook E R, Briffa K R, Meko D M, Graybill D A, Funkhouser G. 1995. The 'segment length curse' in long tree-ring chronology development for palaeoclimatic studies. Holocene, 5: 229–237

Cook E R, Peters K. 1997. Calculating unbiased tree-ring indices for the study of climatic and environmental change. Holocene, 7: 361–370

Dai A. 2013. Increasing drought under global warming in observations and models. Nat Clim Change, 3: 52–58

Deng Y, Gou X, Gao L, Zhao Z, Cao Z, Yang M. 2012. Aridity changes in the eastern Qilian Mountains since AD 1856 reconstructed from tree-rings. Quat Int, 283: 78–84

Diaz H F, Trigo R, Hughes M K, Mann M E, Xoplaki E, Barriopedro D. 2011. Spatial and temporal characteristics of climate in Medieval Times revisited. Bull Amer Meteorol Soc, 92: 1487–1500

Esper J, Cook E R, Krusic P J, Peters K. 2003. Tests of the RCS method for preserving low-frequency variability in long tree-ring chronologies. Tree-Ring Res, 59: 81–98

Esper J, Frank D, Büntgen U, Kirdyanov A. 2009. Influence of pith offset on tree-ring chronology trend. Trace, 7: 205–210

Fang K, Frank D, Zhao Y, Zhou F, Seppä H. 2015. Moisture stress of a hydrological year on tree growth in the Tibetan Plateau and surroundings. Environ Res Lett, 10: 034010

Fang K, Gou X, Chen F, Li J, D'Arrigo R, Cook E, Yang T, Davi N. 2009. Reconstructed droughts for the southeastern Tibetan Plateau over the past 568 years and its linkages to the Pacific and Atlantic Ocean climate variability. Clim Dyn, 35: 577–585

Fritts H C. 1976. Tree Rings and Climate. London: Academic Press

Gou X, Deng Y, Gao L, Chen F, Cook E, Yang M, Zhang F. 2015a. Millennium tree-ring reconstruction of drought variability in the eastern Qilian Mountains, northwest China. Clim Dyn, 45: 1761–1770

Gou X, Gao L, Deng Y, Chen F, Yang M, Still C. 2015b. An 850-year tree-ring-based reconstruction of drought history in the western Qilian Mountains of northwestern China. Int J Climatol, 35: 3308–3319

Graham N E, Ammann C M, Fleitmann D, Cobb K M, Luterbacher J. 2010. Support for global climate reorganization during the "Medieval Climate Anomaly". Clim Dyn, 37: 1217–1245

Holmes R. 1983. Computer assisted quality control in tree-ring dating and measurement. Tree-Ring Bull, 43: 69–78

Huang J, Yu H, Dai A, Wei Y, Kang L. 2017. Drylands face potential threat under 2°C global warming target. Nat Clim Change, 7: 417–422

Huang J, Yu H, Guan X, Wang G, Guo R. 2015. Accelerated dryland expansion under climate change. Nat Clim Change, 6: 166–171

Huang N E, Shen Z, Long S R, Wu M C, Shih H H, Zheng Q, Yen N C, Tung C C, Liu H H. 1998. The empirical mode decomposition and the Hilbert spectrum for nonlinear and non-stationary time series analysis. Proc R Soc Lond Ser A-Math Phys Eng Sci, 454: 903–995

Kang S, Yang B, Qin C. 2012. Recent tree-growth reduction in north central China as a combined result of a weakened monsoon and atmospheric oscillations. Clim Change, 115: 519–536

Li J, Cook E R, D'Arrigo R, Chen F, Gou X. 2008. Moisture variability across China and Mongolia: 1951–2005. Clim Dyn, 32: 1173–1186

Li J, Shi J, Zhang D D, Yang B, Fang K, Yue P H. 2017. Moisture increase in response to high-altitude warming evidenced by tree-rings on the southeastern Tibetan Plateau. Clim Dyn, 48: 649–660

Li Q, Liu Y, Nakatsuka T, Fang K, Song H, Liu R, Sun C, Li G, Wang K. 2018. East Asian Summer Monsoon moisture sustains summer relative humidity in the southwestern Gobi Desert, China: Evidence from $\delta^{18}O$ of tree rings. Clim Dyn, https://doi.org/10.1007/s00382-018-4515-6

Liang E, Shao X, Liu X. 2009. Annual precipitation variation inferred from tree rings since AD 1770 for the Western Qilian Mts., Northern Tibetan Plateau. Tree-Ring Res, 65: 95–103

Liang E, Leuschner C, Dulamsuren C, Wagner B, Hauck M. 2016a. Global warming-related tree growth decline and mortality on the north-eastern Tibetan plateau. Clim Change, 134: 163–176

Liang E, Wang Y, Piao S, Lu X, Camarero J J, Zhu H, Zhu L, Ellison A M, Ciais P, Peñuelas J. 2016b. Species interactions slow warming-induced upward shifts of treelines on the Tibetan Plateau. Proc Natl Acad Sci USA, 113: 4380–4385

Liu Y, An Z, Ma H, Cai Q, Liu Z, Kutzbach J K, Shi J, Song H, Sun J, Yi L, Li Q, Yang Y, Wang L. 2006. Precipitation variation in the northeastern Tibetan Plateau recorded by the tree rings since 850 AD and its relevance to the Northern Hemisphere temperature. Sci China Ser D-Eartn

Sci, 49: 408–420
Liu Y, Sun C, Li Q, Cai Q. 2016. A picea crassifolia tree-ring width-based temperature reconstruction for the Mt. Dongda region, Northwest China, and its relationship to large-scale climate forcing. PLoS ONE, 11: e0160963
Ljungqvist F C, Krusic P J, Brattström G, Sundqvist H S. 2012. Northern Hemisphere temperature patterns in the last 12 centuries. Clim Past, 8: 227–249
Ljungqvist F C, Krusic P J, Sundqvist H S, Zorita E, Brattström G, Frank D. 2016. Northern Hemisphere hydroclimate variability over the past twelve centuries. Nature, 532: 94–98
Melvin T M, Briffa K R. 2008. A "signal-free" approach to dendroclimatic standardisation. Dendrochronologia, 26: 71–86
Melvin T M, Briffa K R. 2014. CRUST: Software for the implementation of regional chronology standardisation: Part 1. Signal-Free RCS. Dendrochronologia, 32: 7–20
Mosley-Thompson E, Thompson L G, Dai J, Davis M, Lin P N. 1993. Climate of the last 500 years: High resolution ice core records. Quat Sci Rev, 12: 419–430
Pederson N, Hessl A E, Baatarbileg N, Anchukaitis K J, Di Cosmo N. 2014. Pluvials, droughts, the Mongol Empire, and modern Mongolia. Proc Natl Acad Sci USA, 111: 4275–4379
Qin C, Yang B, Melvin T M, Fan Z, Zhao Y, Briffa K R. 2013. Radial growth of Qilian Juniper on the Northeast Tibetan Plateau and potential climate associations. PLoS ONE, 8: e79362
Shao X, Liang E, Huang L, Wang L. 2005. A 1437-year precipitation history from Qilian juniper in the northeastern Qinghai-Tibetan Plateau. PAGES news, 13: 14–15
Shao X, Xu Y, Yin Z Y, Liang E, Zhu H, Wang S. 2010. Climatic implications of a 3585-year tree-ring width chronology from the northeastern Qinghai-Tibetan Plateau. Quat Sci Rev, 29: 2111–2122
Sheppard P R, Tarasov P E, Graumlich L J, Heussner K U, Wagner M, wsterle H, Thompson L G. 2004. Annual precipitation since 515 BC reconstructed from living and fossil juniper growth of northeastern Qinghai Province, China. Clim Dyn, 23: 869–881
Tian Q, Gou X, Zhang Y, Peng J, Wang J, Chen T. 2007. Tree-Ring Based Drought Reconstruction (AD 1855–2001) for the Qilian Mountains, Northwestern China. Tree-Ring Res, 63: 27–36
van der Schrier G, Barichivich J, Briffa K R, Jones P D. 2013. A scPDSI-based global data set of dry and wet spells for 1901–2009. J Geophys Res-Atmos, 118: 4025–4048
Wang J, Yang B, Ljungqvist F C, Luterbacher J, Osborn T J, Briffa K R, Zorita E. 2017. Internal and external forcing of multidecadal Atlantic climate variability over the past 1200 years. Nat Geosci, 10: 512–517
Wang J, Yang B, Qin C, Kang S, He M, Wang Z. 2014. Tree-ring inferred annual mean temperature variations on the southeastern Tibetan Plateau during the last millennium and their relationships with the Atlantic Multidecadal Oscillation. Clim Dyn, 43: 627–640
Wang W Z, Liu X H, Xu G B, Shao X M, Qin D H, Sun W Z, An W L, Zeng X M. 2013. Moisture variations over the past millennium characterized by Qaidam Basin tree-ring δ^{18}O. Chin Sci Bull, 58: 3956–3961
Wang Z, Yang B, Deslauriers A, Bräuning A. 2015. Intra-annual stem radial increment response of Qilian juniper to temperature and precipitation along an altitudinal gradient in northwestern China. Trees, 29: 25–34
Wang Z, Yang B, Deslauriers A, Qin C, He M, Shi F, Liu J. 2012. Two phases of seasonal stem radius variations of *Sabina przewalskii* Kom. in northwestern China inferred from sub-diurnal shrinkage and expansion patterns. Trees, 26: 1747–1757
Wigley T M L, Briffa K R, Jones P D. 1984. On the average value of correlated time series, with applications in dendroclimatology and hydrometeorology. J Clim Appl Meteorol, 23: 201–213
Wilson R, Anchukaitis K, Briffa K R, Büntgen U, Cook E, D'Arrigo R, Davi N, Esper J, Frank D, Gunnarson B, Hegerl G, Helama S, Klesse S, Krusic P J, Linderholm H W, Myglan V, Osborn T J, Rydval M, Schneider L, Schurer A, Wiles G, Zhang P, Zorita E. 2016. Last millennium northern hemisphere summer temperatures from tree rings: Part I: The long term context. Quat Sci Rev, 134: 1–18
Wu Z, Huang N E. 2009. Ensemble empirical mode decomposition: A noise assisted data analysis method. Adv Adapt Data Anal, 01: 1–41
Xu G, Yao H, Dong A. 1997. Climate Change in Arid and Semiarid Regions of China (in Chinese). Beijing: China Meteorological Press. 1–101
Yang B, Bräuning A, Johnson K R, Shi Y. 2002. General characteristics of temperature variation in China during the last two millennia. Geophys Res Lett, 29: 1324
Yang B, He M, Melvin T M, Zhao Y, Briffa K R. 2013. Climate control on tree growth at the upper and lower treelines: A case study in the qilian mountains, Tibetan Plateau. PLoS ONE, 8: e69065
Yang B, He M, Shishov V, Tychkov I, Vaganov E, Rossi S, Ljungqvist F C, Bräuning A, Grießinger J. 2017a. New perspective on spring vegetation phenology and global climate change based on Tibetan Plateau tree-ring data. Proc Natl Acad Sci USA, 114: 6966–6971
Yang B, Qin C, Bräuning A, Burchardt I, Liu J. 2011. Rainfall history for the Hexi Corridor in the arid northwest China during the past 620 years derived from tree rings. Int J Climatol, 31: 1166–1176
Yang B, Qin C, Wang J, He M, Melvin T M, Osborn T J, Briffa K R. 2014. A 3500-year tree-ring record of annual precipitation on the northeastern Tibetan Plateau. Proc Natl Acad Sci USA, 111: 2903–2908
Yang B, Sonechkin D M, Datsenko N M, Liu J, Qin C. 2017b. Establishment of a 4650-year-long eigenvalue chronology based on tree-ring cores from Qilian junipers (*Juniperus przewalskii* Kom.) in Western China. Dendrochronologia, 46: 56–66
Yin Z Y, Zhu H, Huang L, Shao X. 2016. Reconstruction of biological drought conditions during the past 2847 years in an alpine environment of the northeastern Tibetan Plateau, China, and possible linkages to solar forcing. Glob Planet Change, 143: 214–227
Zhang P, Cheng H, Edwards R L, Chen F, Wang Y, Yang X, Liu J, Tan M, Wang X, Liu J, An C, Dai Z, Zhou J, Zhang D, Jia J, Jin L, Johnson K R. 2008. A test of climate, sun, and culture relationships from an 1810-year chinese cave record. Science, 322: 940–942
Zhang Q B, Cheng G, Yao T, Kang X and Huang J. 2003. A 2,326-year tree-ring record of climate variability on the northeastern Qinghai-Tibetan Plateau. Geophys Res Lett, 30: 1739–1742
Zhang Q B, Evans M N, Lyu L. 2015. Moisture dipole over the Tibetan Plateau during the past five and a half centuries. Nat Commun, 6: 8062
Zhang Y, Shao X, Yin Z, Liang E, Tian Q, Xu Y. 2011. Characteristics of extreme droughts inferred from tree-ring data in the Qilian Mountains, 1700−2005. Clim Res, 50: 141–159

(Responsible editor: Yan ZHAO)